Research article

Journal of MASS SPECTROMETRY

Received: 3 April 2014 Revised: 6 August 2014 Accepted: 7 August 2014 Published online in Wiley Online Library

(wileyonlinelibrary.com) DOI 10.1002/jms.3463

Measuring oxygen yields of a thermal conversion/elemental analyzer-isotope ratio mass spectrometer for organic and inorganic materials through injection of CO

Xijie Yin[a] and Zhigang Chen[b]*

The thermal conversion/elemental analyzer-isotope ratio mass spectrometer (TC/EA-IRMS) is widely used to measure the $\delta^{18}O$ value of various substances. A premise for accurate $\delta^{18}O$ measurement is that the oxygen in the sample can be converted into carbon monoxide (CO) quantitatively or at least proportionally. Therefore, a precise method to determine the oxygen yield of TC/EA-IRMS measurements is needed. Most studies have used the CO peak area obtained from a known amount of a solid reference material (for example, benzoic acid) to calibrate the oxygen yield of the sample. Although it was assumed that the oxygen yield of the solid reference material is 100%, no direct evidence has been provided. As CO is the analyte gas for $\delta^{18}O$ measurement by IRMS, in this study, we use a six-port valve to inject CO gas into the TC/EA. The CO is carried to the IRMS by the He carrier gas and the CO peak area is measured by the IRMS. The CO peak area thus obtained from a known amount of the injected CO is used to calibrate the oxygen yield of the sample. The oxygen yields of commonly used organic and inorganic reference materials such as benzoic acid (C_6H_5COOH), silver phosphate (Ag_3PO_4), calcium carbonate ($CaCO_3$) and silicon dioxide (SiO_2) are investigated at different reactor temperatures and sample sizes. We obtained excellent linear correlation between the peak area for the injected CO and its oxygen atom amount. C_6H_5COOH has the highest oxygen yield, followed by Ag_3PO_4, $CaCO_3$ and SiO_2. The oxygen yields of TC/EA-IRMS are less than 100% for both organic and inorganic substances, but the yields are relatively stable at the specified reactor temperature and for a given quantity of sample. Copyright © 2014 John Wiley & Sons, Ltd.

Keywords: organic and inorganic oxygen yield; on-line; thermal conversion; pyrolysis; IRMS

Introduction

Oxygen is the most abundant element in the Earth's crust and exists in a variety of substances in gaseous (for example, O_2 and water vapor), liquid (for example, water, oxygen-containing ions and dissolved organic matters) and solid forms (for example, various organic and inorganic solid matters). Oxygen is involved in one way or another in most life processes and plays key roles in the biogeochemical cycling of other elements such as carbon, nitrogen and sulfur. It has three isotopes, ^{16}O, ^{17}O and ^{18}O, which are valuable tracers for processes involving oxygen. Oxygen isotopes have been studied for years[1] and successfully used as tracers in paleoclimatology, ecology, geology, physiology, biochemistry, agriculture and forensic science.[2,3]

Oxygen exists in a variety of substances and forms, many suitable methods have been established to measure its $\delta^{18}O$ values.[4,5] For carbonate samples, the most common method is reaction with water free phosphoric acid and then to mass spectrometrically measure the released CO_2.[6] For water samples, the classical method is equilibration with CO_2 of known isotopic compositions in the headspace.[7,8] Likewise, fluorination is the most widely used method for compounds with a high decomposition temperature (for example, silicates and oxides),[9] and a large variety of methods have been developed to measure the $\delta^{18}O$ value of organic matter including heating the sample material together with either $HgCl_2$ or $Hg(CN)_2$[10,11] pyrolysis in a Ni tube [12] or reduction with carbon at high temperatures.[13,14] For historical reasons, international oxygen isotope reference materials are either carbonate or water. Only two methods, namely, the phosphoric acid reaction method for carbonates and the H_2O–CO_2 equilibration method for water samples, are considered standard methods. However, when carbonates react with phosphoric acid, the oxygen in the carbonate is only partially converted to CO_2, whereas during the H_2O–CO_2 equilibration, the oxygen isotopic fractionation factor between H_2O and CO_2 depends on the temperature. All other non-standard methods normally involve complex operation and hazardous reagents (for example, BrF_5 or BrF_3) and are for special purposes and samples only. Most importantly, these non-standard methods cannot measure international oxygen isotope reference materials (carbonate or water) directly, which create difficulties in comparing the $\delta^{18}O$ values among different materials and laboratories. The key problem is therefore the lack of method that can convert the oxygen in various types of substances to a common light gas, which can serve as the measurement gas, either quantitatively or at least proportionally.

* Correspondence to: Zhigang Chen, College of Ocean and Earth Sciences, Xiamen University, Xiamen, 361102, China. E-mail: chzhg@xmu.edu.cn

a Third Institute of Oceanography, State Oceanic Administration, Xiamen, Fujian, 361005, China

b College of Ocean and Earth Sciences, Xiamen University, Xiamen, Fujian, 361102, China

Journal of MASS SPECTROMETRY

In recent years, more studies have used thermal conversion/elemental analyzer-isotope ratio mass spectrometer (TC/EA-IRMS) to measure the $\delta^{18}O$ value of different substances. Other acronyms that refer to TC/EA (thermal conversion/elemental analyzer) include high-temperature conversion, high-temperature pyrolysis, high-temperature carbon reduction.[15] TC/EA is in principle similar to the carbon reduction method. [13,14] The TC/EA-IRMS measurement of the $\delta^{18}O$ value is performed on-line by pyrolyzing the sample at high temperature (up to 1450 °C) and convert the oxygen in the sample into CO at high temperature. The generated CO is carried into IRMS through an open-split interface by the carrier gas.[16,17] The precision of TC/EA-IRMS is in general close to or slightly lower than other methods, but it has the combined advantages of minimal sample amount requirement, easy operation, high throughput, and most importantly, the capability to measure the $\delta^{18}O$ value of different types of substances. These advantages make the $\delta^{18}O$ value comparison among different laboratories and substances feasible.[15] The substances whose $\delta^{18}O$ value can be measured by TC/EA-IRMS include organic matter,[2,16,18,19] phosphate,[20–22] sulfate,[23–26] nitrate,[27,28] water,[15,29,30] as well as carbonates, oxides and silicates.[3,5,17,26,30,31]

The premise of accurate $\delta^{18}O$ measurement is that the oxygen in the samples can be converted completely or proportionally into the analyte gas (CO_2 or CO) before being measured by mass spectrometry.[17,32] Low oxygen yield may cause isotopic fractionation. Reactor temperature and sample size are the controlling factors to oxygen yield. It is believed that the higher the reactor temperature is, the higher oxygen yield of the TC/EA method can be achieved. However, with the increase in reactor temperature, the measurement background also increases and the reactor lifetime is compromised.[33] When the sample size is too small, the measurement precision deteriorates, whereas large samples may lead to incomplete pyrolysis. The carbon reduction method was first used to measure the oxygen content of organic matter, [34. 35] and the oxygen yield was determined by measuring the amount of formed CO_2 directly either manometrically, volumetrically, iodometrically or gravimetrically.[34–36] As these methods are very cumbersome, and inaccurate, they were rarely used in recent years. The oxygen yield of the TC/EA–IRMS method is rarely examined adequately. Most of the published work uses the CO peak area obtained from a known amount of solid reference material (e.g. C_6H_5COOH) to calibrate the oxygen yield of the sample. These methods assume that the oxygen yield of the solid reference material is 100%,[17,20,26,31,37,38] which has not yet been proven.

Because CO is the analyte gas of the $\delta^{18}O$ measurement by TC/EA–IRMS, the oxygen in the samples first needs to be converted to CO through TC/EA. So, the most precise method to measure the oxygen yield of TC/EA-IRMS is to use CO as the reference material. Therefore, in this study, we inject a certain volume of CO gas into TC/EA by a six-port valve and used the CO peak area obtained from a known amount of the injected CO to calibrate the oxygen yield of the sample. Using this method, the oxygen yield of C_6H_5COOH, Ag_3PO_4, $CaCO_3$ and SiO_2 is studied at different temperatures and sample sizes. We report the oxygen yield results in this paper. The associated $\delta^{18}O$ value results will be reported in a companion paper.

Experimental

The injected CO gas is the same as the reference gas (99.9999%), and the carrier gas is He (99.9999%). Ag_3PO_4 was purchased from Alfa Aesar (99%), C_6H_5COOH from HEKAtech GmbH (Cat #: 02432–493649), $CaCO_3$ from Merck KGaA (B0391759025, 99.95%) and SiO_2 from the Tianjin Guangfu Fine Chemical Research Institute (spectrometry grade purity). Silver capsules are obtained from SANTIS (SA76980506, 3.3 × 5.0 mm). The six-port valve is the manual operation type of VICI (MNK250414) and the volume of the sample loops is 50, 100, 250 and 500 μl, respectively. The model of TC/EA-IRMS is Flash HT-Delta V Advantage (Thermo Fisher), [Figs. 1(d, e and f)]. Following each instrument restart or reactor temperature change, measurement of sample $\delta^{18}O$ was attempted only after the standard deviation of the repeated $\delta^{18}O$ measurement of reference gas is better than 0.06‰.

The TC/EA used for the work reported here is in the standard configuration. The heart of the TC/EA is a high-temperature reactor [Fig. 1(d)], which is mainly composed of an outer ceramic tube and an inner glassy carbon tube. The glassy carbon is a very inert material,[5,18] virtually free of oxygen,[16] has no long range order and is made from the thermal decomposition of a 3D cross-linked synthetic resin.[29] Outside the ceramic tube is the heating resistor, which provides the controllable high temperature. At the bottom of the ceramic tube is a layer of silver filament; on top of the silver filament is a layer of silica wool, which is covered with a layer of glassy carbon grit (diameter ≈ 3 mm). The glassy carbon tube is placed on the glassy carbon grit. The glassy carbon tube is filled with a layer of silver filament at the bottom and then a layer of glassy carbon grit. A graphite crucible is placed on top of the glassy carbon grit to carry the reaction residue. By adjusting the amount of glassy carbon grit in the glassy carbon tube, the crucible can be precisely positioned at the hottest zone. After every 70 measurements, the reactor temperature is lowered to 500 °C and the crucible is taken out and emptied.

The carrier gas enters the system from the top of the reactor and a portion of the gas flows down through the glassy carbon tube, whereas the rest flows down through the gap between the glassy carbon tube and the ceramic tube. When the solid sample falls into the high-temperature glassy carbon tube, the oxygen atoms in the sample are converted to CO. The CO is carried out of the reactor by the carrier gas to a 5-Å molecular sieve GC column (1.0 m), where it is separated from N_2 and other gases. The CO flows into the IRMS via an open-split interface [Fig. 1(e)] to measure the CO peak area [Fig. 1(g)]. The flow rate of the carrier gas is 60 ml/min and the temperature of the GC column is 95 °C.

For solid sample analysis, powdered samples of different sizes were weighed into silver capsules. The tightly folded capsules were then placed on a No Blank Autosampler (AS2000, Thermo Fisher), [Fig. 1(c)], which is continually purged with He to eliminate any trace of water, oxygen and nitrogen. Under the control of software (ISODAT3.0), the No Blank AutoSampler drops the sample capsules into the high-temperature reactor. Measurement with empty silver capsule showed its *m/z* 28 peak intensity <2 mV, which means that the silver capsule nearly do not contain oxygen.

For the CO injection experiment, the No Blank Autosampler is alternated by a six-port valve with a sample loop [Fig. 1(a, b)]. The six-port valve is connected to the TC/EA in two ways. First is the 'shallow injection' technique [Fig. 1(d1)], the top of the ceramic tube is sealed by a nut with a side air vent, the six-port valve is connected to the air vent and both CO and carrier gases come into the reactor through the air vent. In this way, most of the injected CO flows through the glassy carbon tube, whereas the rest flows through the gap between the ceramic tube and the glassy carbon tube. Second is the 'deep injection' technique [Fig. 1(d2)], the top of the ceramic tube is sealed by a nut, which is usually used to inject

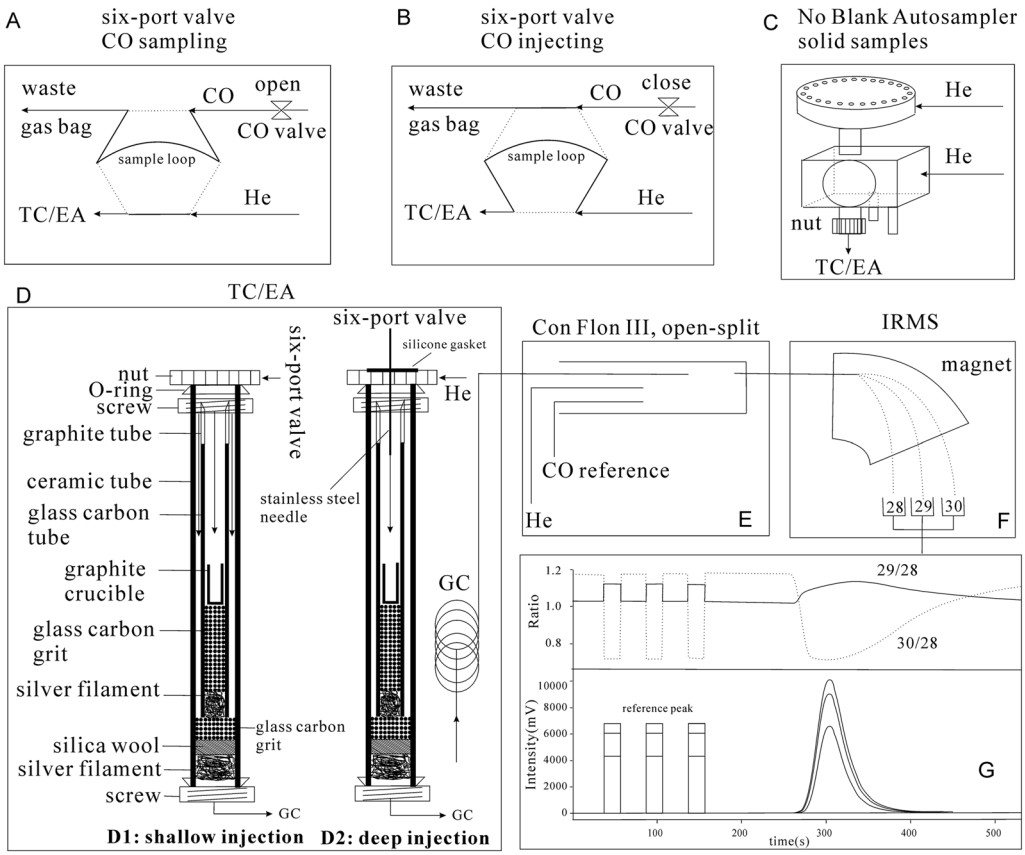

Figure 1. The configuration of TC/EA-IRMS. The arrows in the tube (reactor) represent the flow direction of the CO.

liquid samples. This nut has a side air vent too, but the top of it is sealed by a silicone gasket. The six-port valve is connected to the TC/EA by a stainless steel needle (OD = 1 mm), which penetrates the silicone gasket, and goes deep into the glassy carbon tube. CO is injected deep into the glassy carbon tube through the stainless steel needle at a flow rate of 5 ml/min; the carrier gas flows into the reactor mostly through the air vent at a flow rate of 55 ml/min. In this way, the injected CO only flows through the glass carbon tube. In both connection ways, the six-port valve is also connected to the He carrier gas cylinder and CO reference gas cylinder. A CO valve is connected between the CO cylinder and the six-port valve. After the third reference peak is eluted [Fig. 1(g)], the CO valve is first opened to fill the sample loop with CO [Fig. 1(a)]; after that, the CO valve is closed and the six-port valve is switched on immediately, allowing the carrier gas to flush the CO from the sample loop into the high-temperature reactor [Fig. 1(b)]. An empty airbag is connected to the CO vent of the six-port valve to collect the toxic surplus CO.

The oxygen atom amount in the injected CO is calculated by dividing the injected volume with the molar volume of the gas (24.46 l/mol at 25 °C). Combined with the measured peak area, the relationship between the CO peak area of the injected CO and its oxygen atom amount can be established (refer to as 'CO formula' hereafter). Putting the measured CO peak area of the sample into the CO formula, the measured oxygen atom amounts of the sample are obtained. From the mass and molecular mass of the sample, its actual oxygen atom amounts can be calculated. Dividing the measured oxygen atom amounts by the actual oxygen atom amounts of the sample, the oxygen yield of the sample is obtained.

Results and discussion

Oxygen yield of the injected CO

Figure 2 shows the relationship between the peak area of the injected CO and the reactor temperature at four injection volumes: 50, 100, 250 and 500 µl. For the 'shallow injection' technique [Fig. 1(d1)], it is clear that the CO peak area is

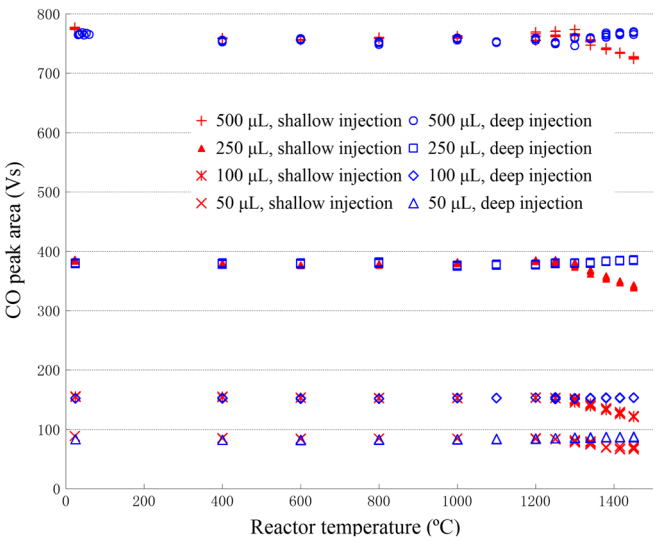

Figure 2. The relationship between measured CO peak area and reactor temperature for the CO injection experiments.

Journal of MASS SPECTROMETRY

stable at reactor temperature between 25 and 1250 °C. When the reactor temperature increases from 1250 to 1450 °C, CO peak area steadily decreases. These changes imply that CO loss happens when the reactor temperature exceeds 1250 °C, and the higher the reactor temperature is, the more CO is lost. We hypothesize that such CO loss may occur in the gap between the ceramic tube and the glassy carbon tube. To test this hypothesis, we used the 'deep injection' technique [Fig. 1(d2)] to ensure that all CO flows through the glassy carbon tube. Figure 2 shows that the peak areas of the deep injected CO are stable for all temperatures. Thus, it is clear that beyond 1250 °C, the loss of CO most likely occurred through the gap between the ceramic and glass carbon tubes. The CO loss in the gap can occur via (1) direct leakage and (2) reaction with the reactor. We tend to accept the former explanation because, under high-temperature conditions, the ceramic tube can expand and its gas tightness diminishes. As both the total gas pressure and CO partial pressure in the gap are higher than those of the outside, some of the CO may penetrate the ceramic tube wall and lose to the outside. Although this explanation is contrary to the conventional opinion that the air will penetrate into the ceramic tube at higher temperature, [[27]] it is consistent with the fact the loss of CO beyond 1250 °C is predictably much weaker for the two solid samples C_6H_5COOH and Ag_3PO_4, as CO formed from solids only flows through the glassy carbon tube.

With the results obtained from the 'deep injection' technique at the tested reactor temperature between 25 and 1450 °C, we established the relationship (the CO formula) between the oxygen atom amount and peak area of the injected CO.

$$y = 36.9717x + 5.7932 \quad (1)$$

where y is the CO peak area (Vs), and x is the oxygen atom amount (μmol). The R^2 for the correlation is highly significant 0.9997 ($P < 0.0001$, $n = 287$), (Figs. 3, 5 and 7).

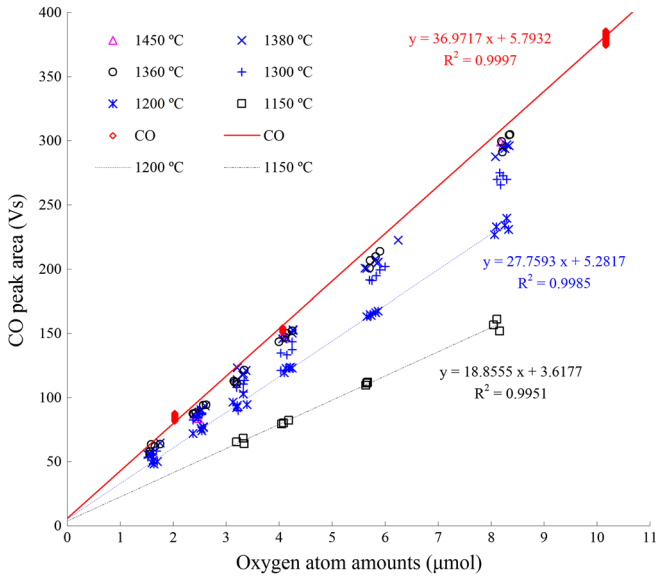

Figure 3. The relationship between the oxygen atom amounts of C_6H_5COOH and CO peak area at different reactor temperatures. The oxygen atom amounts of C_6H_5COOH are calculated from its mass and molecular mass. The legend with CO represents the results of CO deep injection experiment, all others with temperatures represent C_6H_5COOH measured at that temperature. For clarity, the data points of the CO injection volume of 500 μl are not shown but were used for the generation of the fitted line and the CO formula (see also in Figures 5 and 7).

We then use the CO formula to calibrate the oxygen yields of the solid samples. If the oxygen atoms in the solid samples are completely converted to CO, the respective data points should fall on the fitted line of the injected CO.

Oxygen yield of C_6H_5COOH

Figure 3 shows the relationship between the measured CO peak area and the oxygen atom amount of C_6H_5COOH, which is calculated from the mass and molecular mass of C_6H_5COOH. It is evident that when the reactor temperature exceeds 1360 °C, C_6H_5COOH has the largest CO peak area, and the data points fall closer to the fitted line of the injected CO. With the decrease of reactor temperature, the slope of the fitted line decreases too. Figure 4 shows the relationship between the reactor temperature and the oxygen yield of C_6H_5COOH. It reveals that the oxygen yields at 1450, 1380 and 1360 °C are similar, with average values of 92.8%, 91.9% and 92.8%, respectively. However, with the decrease in reactor temperature, the oxygen yields decrease significantly from an average value of 85.8% at 1300 °C to 74.6% at 1200 °C and 49.8% at 1150 °C (Table 1). The results show that oxygen from C_6H_5COOH is not completely converted to CO even at 1450 °C.

Oxygen yield of Ag_3PO_4

Figure 5 shows the relationship between the measured CO peak area and the oxygen atom amount of Ag_3PO_4, which is calculated from the mass and molecular mass of Ag_3PO_4. It is clear that when the reactor temperature is higher than 1300 °C, Ag_3PO_4 has the largest CO peak area, and the slopes of the fitted lines are similar to each other. However, all Ag_3PO_4 data points still fall below the fitted line of the injected CO. With the decrease of reactor temperature, the slope of the fitted line decreases too. Figure 6 shows the relationship between the reactor temperature and oxygen yield of Ag_3PO_4. We can see that except for 1340 °C, the oxygen yields of Ag_3PO_4 decrease gradually with the decrease of reactor temperature. The oxygen yields from 0.2 mg are clearly low and variable, so the data for 0.2 mg were removed when calculating the average oxygen yield of Ag_3PO_4 (Table 1). The average oxygen

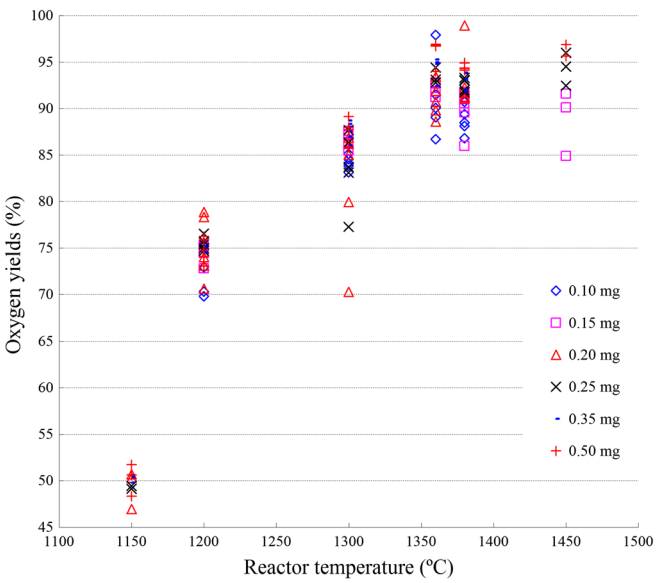

Figure 4. The relationship between the oxygen yield of C_6H_5COOH and the reactor temperature.

Table 1. Average oxygen yields of samples at different reactor temperatures

Sample	Oxygen yield (%)[a]								
	1450 °C	1415 °C	1380 °C	1360 °C	1340 °C	1300 °C	1250 °C	1200 °C	1150 °C
C_6H_5COOH	92.8 (4.3, 8)[b]	—	91.9 (2.8, 32)	92.8 (2.9, 27)	—	85.8 (3.0, 30)	—	74.6 (2.7, 30)	49.8 (2.5, 12)
Ag_3PO_4	89.8 (3.2, 24)	88.7 (4.0, 25)	86.0 (3.6, 25)	—	89.7 (3.0, 25)	82.0 (4.9, 25)	82.6 (2.8, 25)	73.3 (4.0, 25)	64.0 (2.7, 3)
$CaCO_3$	61.1 (7.4, 25)	—	—	—	—	—	—	—	—
SiO_2	<2	—	—	—	—	—	—	—	—

[a]The oxygen yield is the average of different masses.
[b]The first number in parentheses is the RSD (%), and the second one is the number of the samples.

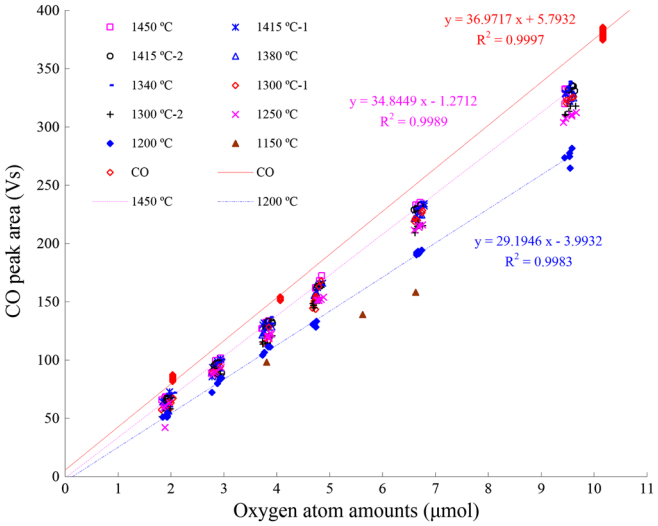

Figure 5. The relationship between the oxygen atom amounts of Ag_3PO_4 and CO peak area at different reactor temperatures. The oxygen atom amounts of Ag_3PO_4 are calculated from its mass and molecular mass. The legend with CO represents the results of CO deep injection experiment, all others with temperatures represent Ag_3PO_4 measured at that temperature. For clarity, the data points of the CO injection volume of 500 μl are not shown but were used for the generation of the fitted line and the CO formula (Figures 3 and 7).

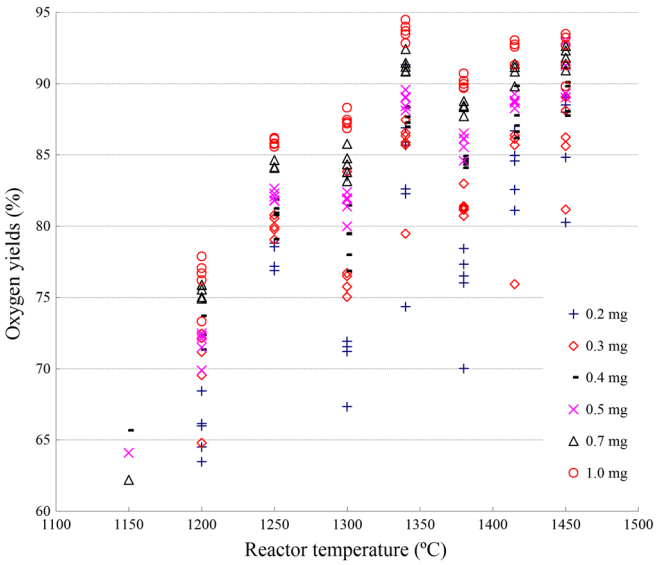

Figure 6. The relationship between the oxygen yield of Ag_3PO_4 and the reactor temperature.

yields of Ag_3PO_4 at different reactor temperatures are as follows: 89.8% (1450 °C), 88.7% (1415 °C), 86.0% (1380 °C), 89.7% (1340 °C), 82.0% (1300 °C), 82.6% (1250 °C), 73.3% (1200 °C) and 64.0% (1150 °C). The exact cause of the higher oxygen yield at 1340 °C is unclear at this stage. Some earlier studies using benzoic acid (C_6H_5COOH) as the reference material and assuming an oxygen yield of 100% for it obtained an oxygen yield of 90–100% for Ag_3PO_4 at 1450 °C. [[38]] Likewise, Vennemann *et al.* [20] obtained an oxygen yield of 100% for Ag_3PO_4 and KH_2PO_4 at 1450 °C, but it decreased to 90% when the crucible was filled with residue or when the reactor temperature decreased to 1400 °C.

Journal of MASS SPECTROMETRY

Oxygen yields of $CaCO_3$ and SiO_2

As both $CaCO_3$ and SiO_2 are hard to pyrolyze, we studied the oxygen yield of $CaCO_3$ and SiO_2 at the highest designed temperature of the TC/EA (1450 °C). Figure 7 shows that the data points of $CaCO_3$ (star) fall below the fitted line of injected CO. It is clear that the oxygen atoms of $CaCO_3$ are not completely converted to CO. If we assume that only 2/3 of oxygen atoms in $CaCO_3$ is converted to CO, then the recalculated results (shown as black triangle in Fig. 7) are very close to the fitted line of the injected CO. This implies that about 2/3 of the oxygen atoms in $CaCO_3$ is converted to CO at 1450 °C and the remaining 1/3 of oxygen atoms probably exists in CaO, indicating a decomposition of $CaCO_3$ at 1450 °C to CO and CaO via $CaCO_3 + C(\text{from glassy carbon}) \rightarrow CaO + 2CO$. The calculated average oxygen yield of $CaCO_3$ at 1450 °C is 61.1%. If no oxygen isotope fractionation or only a stable isotope fractionation factor is involved in this decomposition process, the $\delta^{18}O$ value of carbonate can be directly measured by TC/EA-IRMS without any additives. Boschetti and Iacumin [26] using benzoic acid as the reference material obtained an oxygen yield of 67% for $CaCO_3$ at 1400 °C, but when using AgCl as an additive, the value increased to 101–108% at a reactor temperature of 1420 °C. Crowley *et al.* [31] used AgCl as an additive and used nitrate salts as the reference material, obtained an oxygen yields of 77.0 ~ 104.5% for carbonate, with a mean value of 93.6% at 1420 °C and 85.45% at 1500 °C. However, eliminating the potential oxygen contamination from the additives is a challenge for TC/EA-IRMS.

The open squares at the bottom of Fig. 7 represent the results for SiO_2. It is clear that only a small percentage of the oxygen in SiO_2 is converted to CO. The calculated oxygen yield of oxygen from SiO_2 at 1450 °C is lower than 2.0%. Thus, the $\delta^{18}O$ value of silicate and SiO_2 cannot be directly determined by TC/EA-IRMS. Using sucrose as a reference material, Kornexl *et al.* [17] obtained oxygen yields of 87%, 67% and <10% for Ag_3PO_4, $CaCO_3$ and SiO_2, respectively at 1400 °C.

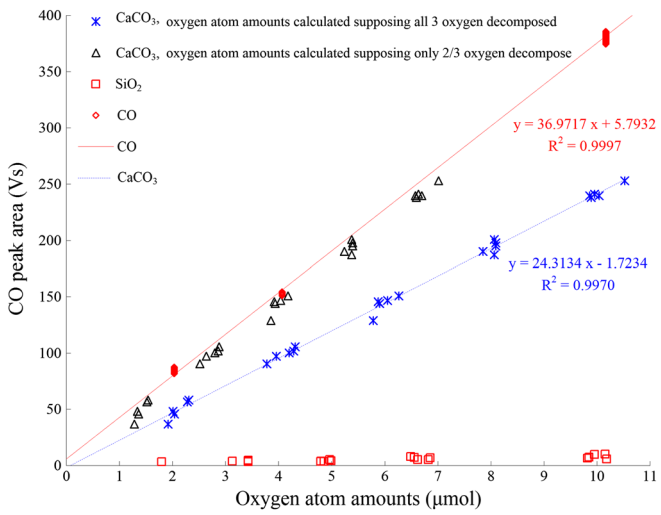

Figure 7. The relationship between the measured CO peak areas and the oxygen atom amounts of $CaCO_3$ and SiO_2 at 1450 °C. The oxygen atom amounts of $CaCO_3$ and SiO_2 are calculated from their mass and molecular mass. For clarity, the data points of the CO injection volume of 500 μl are not shown but were used for the generation of the fitted line and the CO formula (Figures 3 and 5).

The relationship between the oxygen yield and sample size

Figure 6 shows, except for the reactor temperature of 1150 °C, the oxygen yield of Ag_3PO_4 increases with increase in sample size at a given temperature, but this is not evident in the case of C_6H_5COOH (Fig. 4). The difference is likely to be caused by some CO loss for Ag_3PO_4.

As all of the oxygen yields are calculated using the CO formula (Eqn (1)), we can deduce from the geometry that, in Figs. 3, 5 and 7, if the fitted line of the sample at a certain temperature has the same *X*-axis intercept as that of the injected CO, their calculated oxygen yields should not change with sample size. For example, if the *X*-axis intercept is larger than that of the injected CO, this means that CO loss occurred, and the difference between the intercepts of the sample and that of the injected CO is the amount of lost CO. This can lead to the calculated oxygen yield increases with the increase of sample size.

From Figs. 3, 5 and 7, we can see that the difference in the *X*-axis intercept between the fitted lines of the injected CO and the samples measured at 1450 °C decreased in the order $CaCO_3$ $Ag_3PO_4 >$ and C_6H_5COOH. Their CO losses have the same trend, with values of 0.227, 0.193 and −0.034 μmol, respectively. So the oxygen yield of Ag_3PO_4 has a more obvious relationship with the sample size than that of C_6H_5COOH. We have mentioned before that some shallow-injected CO maybe lost by penetrating the ceramic tube when the reactor temperature is higher than 1250 °C. For solid samples, the folded samples fall into the glassy carbon tube, so that the amount of lost CO for solid samples is much less than that of the shallow-injected CO. The exact cause for the difference among C_6H_5COOH, Ag_3PO_4 and $CaCO_3$ is still unclear. It could be that a small percentage of oxygen may exist in a form other than CO under the used pyrolytic conditions due to the presence of elements other than C, H and O in the samples. If this is indeed the case, such loss of O should be elemental composition-dependent.

It should be mentioned that this kind of CO loss for Ag_3PO_4 is mechanistically different from the incomplete decomposition of the sample although both can decrease the CO yield. We will show in the next section that at a given reactor temperature, the proportions of sample decomposed are same for all sample sizes, so that the oxygen yield should not vary with sample size if no CO is lost.

Factors that influence the oxygen yield

From Figs. 3, 5 and 7, we can see that, for all types of samples tested here, the slope of the fitted line decreases with the decrease of the reactor temperature; but for a given reactor temperature, the linearity of the fitted line does not change with the sample size. This suggests that, in the range of the sample size used, the key factor affecting the oxygen yield is the reactor temperature, not the sample size. That is to say that even though the apparent oxygen yield decreases with the decrease of the reactor temperature, within the tested mass range, the samples were still decomposed proportionally at a given temperature. It should be mentioned that for the Ag_3PO_4, the sample size may have an effect at 1150 °C (Figs. 5 and 6).

Under the highest designed temperature of the TC/EA reactor (1450 °C), nearly 2/3 of oxygen in $CaCO_3$ is converted to CO with the remaining 1/3 maybe existing as CaO for Ca–O that has a high bond energy (383.3 ± 5.0 kJ/mol, all bond energies cited in this paper are from [39]). However, the oxygen yield of SiO_2 is <2%, presumably because of the strong bond of Si–O (799.6 ± 13.4 kJ/mol),

which allows only for a very small percentage of oxygen to be released at 1450 °C. Therefore, the ideal substance for $\delta^{18}O$ value measurement by TC/EA-IRMS should not contain high-energy X–O bonds other than CO, which has bond energy of 1076.38 ± 0.67 kJ/mol. Because the Ag–O bond has relatively lower bond energy (221 ± 21 kJ/mol) and Ag_3PO_4 is less hygroscopic, measurements of $\delta^{18}O$ value of phosphate usually involve conversion of the phosphate in the sample into Ag_3PO_4 before being analyzed by TC/EA-IRMS.

These results show that although the oxygen yields of C_6H_5COOH and Ag_3PO_4 are relatively higher than that of $CaCO_3$ and SiO_2, they are still less than 100%. So if C_6H_5COOH is to be used as a reference material to calibrate the oxygen yield of Ag_3PO_4 or other types of samples, an overestimation of oxygen yield is predicted.

Conclusions

In this study, we used CO as a reference material to calibrate the oxygen yields of TC/EA-IRMS for both inorganic and organic materials at different sample sizes and reactor temperatures. On the basis of the results obtained, we conclude that

(1) The oxygen atom amount of injected CO has a good linear correlation with its measured peak area;
(2) When CO flows through the gap between the ceramic tube and the glassy carbon tube at the temperature higher than 1250 °C, CO loss (to the outside of the ceramic tube) occurred. The amount of CO loss increases with the reactor temperature. Minimal CO loss is observed with solid samples or deep injection of CO into the glassy carbon tube;
(3) For a given set of pyrolytic conditions, C_6H_5COOH has the highest oxygen yield, followed by Ag_3PO_4, $CaCO_3$ and SiO_2 in decreasing order;
(4) In the range of sample sizes tested, the key factor that affects the oxygen yield is the reactor temperature rather than the sample size. The X–O bond energy in the sample is another important factor that influences the oxygen yield;
(5) The oxygen yields of TC/EA-IRMS are less than 100% for both organic and inorganic substances, but the yields are relatively stable at a specific reactor temperature and sample size.

Acknowledgements

This study was supported by the Natural Science Foundation of China (No. 41006072, 41276059, 40706033) and the Scientific Research Foundation of the Third Institute of Oceanography (No. 2013019). We gratefully acknowledge the kind help from Drs. Youping Zhou and S. Kandasamy who significantly improved both the English and the quality of the manuscript. Mr. Fan Zhang helped with the TC/EA-IRMS instrumentation.

References

[1] W. F. Giauque, H. L. Johnston. An isotope of oxygen, mass 18. *Nature*. **1929**, *123*, 318.
[2] G. D. Farquhar, B. K. Henry, J. M. Styles. A rapid on-line technique for determination of oxygen isotope composition of nitrogen-containing organic matter and water. *Rapid Commun. Mass Spectrom.* **1997**, *11*, 1554.
[3] R. A. Werner. The online $^{18}O/^{16}O$ analysis: development and application. *Isot. Environ. Health Stud.* **2003**, *39*, 85.
[4] P. A. De Groot. *Handbook of Stable Isotope Analytical Techniques (Vol. 2)*, Elsevier Science: Amsterdam, **2009**.
[5] B. E. Kornexl, R. A. Werner, M. Gehre. Standardization for oxygen isotope ratio measurement-still an unsolved problem. *Rapid Commun. Mass Spectrom.***1999**, *13*, 1248.
[6] J. McCrea. On the isotopic chemistry of carbonates and a paleotemperature scale. *J. Chem. Phys.* **1950**, *18*, 849.
[7] M. Cohn, H. Urey. Oxygen exchange reactions of organic compounds and water. *J. Am. Chem. Soc.* **1938**, *60*, 679.
[8] S. Epstein, T. Mayeda. Variation of ^{18}O content of waters from natural sources. *Geochim. Cosmochim. Acta.* **1953**, *4*, 213.
[9] R. N. Clayton, T. Mayeda. The use of bromine pentafluoride in the extraction of oxygen from oxides and silicates for isotopic analysis. *Geochim. Cosmochim. Acta.* **1963**, *27*, 43.
[10] D. Rittenberg, L. Ponticorvo. A method for the determination of the ^{18}O concentration of the oxygen of organic compounds. *Int. J. Appl. Radiat. Isot.* **1956**, *1*, 208.
[11] J. S. Lee. Determination of ^{18}O concentration of sugars and glycogen. *Anal. Chem.* **1962**, *34*, 835.
[12] P. Thompson, J. Gray. Determination of $^{18}O/^{16}O$ ratios in compounds containing C, H and O. *Int. J. Appl. Radiat. Isot.* **1977**, *28*, 411.
[13] J. Santrock, J. M. Hayes. Adaptation of the Unterzaucher procedure for determination of oxygen-18 in organic substances. *Anal. Chem.* **1987**, *59*, 119.
[14] J. W. Taylor, I. J. Chen. Variables in oxygen-18 isotopic analysis by mass spectrometry. *Anal. Chem.* **1970**, *42*, 224.
[15] W. A. Brand, T. B. Coplen, A. T. Aerts-Bijma, J. K. Böhlke, M. Gehre, H. Geilmann, M. Gröning, H. G. Jansen, H. A. J. Meijer, S. J. Mroczkowski, H. Qi, K. Soergel, H. Stuart-Williams, S. M. Weise, R. A. Werner. Comprehensive inter - laboratory calibration of reference materials for $\delta^{18}O$ versus VSMOW using various on - line high - temperature conversion techniques. *Rapid Commun. Mass Spectrom.* **2009**, *23*, 999.
[16] J. Koziet. Isotope ratio mass spectrometric method for the on-line determination of oxygen-18 in organic matter. *J. Mass Spectrom.* **1997**, *32*, 103.
[17] B. E. Kornexl, M. Gehre, R. Hofling, R. A. Werner. On-line ^{18}O measurement of organic and inorganic substances. *Rapid Commun. Mass Spectrom.* **1999**, *13*, 1685.
[18] R. A. Werner, B. E. Kornexl, A. Roßmann, H. L. Schmidt. On-line determination of $\delta^{18}O$ values of organic substances. *Anal. Chim. Acta.* **1996**, *319*, 159.
[19] O. Bréas, C.Guillou, F. Reniero, E. Sada, F. Angerosa. Oxygen - 18 measurement by continuous flow pyrolysis/isotope ratio mass spectrometry of vegetable oils. *Rapid Commun. Mass Spectrom.* **1998**, *12*, 188.
[20] T. W. Vennemann, H. C. Fricke, R. E. Blake, J. R. O'Neil, A. Colman. Oxygen isotope analysis of phosphates: a comparison of techniques for analysis of Ag_3PO_4. *Chem. Geol.* **2002**, *185*, 321.
[21] C. Lécuyer, F. Fourel, F. Martineau, R. Amiot, A. Bernard, V. Daux, G. Escarguel, J. Morrison. High - precision determination of ^{18}O ratios of silver phosphate by EA - pyrolysis - IRMS continuous flow technique. *J. Mass Spectrom.* **2007**, *42*, 36.
[22] D. F. LaPorte, C. Holmden, W. P. Patterson, T. Prokopiuk, B. M. Eglington. Oxygen isotope analysis of phosphate: improved precision using TC/EA CF-IRMS. *J. Mass Spectrom.* **2009**, *44*, 879.
[23] R. E. Blake, A.V. Surkov, M. E. Böttcher, T. G. Ferdelman, B. B. Jørgensen. Oxygen isotope composition of dissolved sulfate in deep-sea sediments: eastern equatorial Pacific Ocean. *Proc. ODP Sci. Results*. **2006**, *201*, 1.
[24] A. V. Turchyn, V. Brüchert, T. W. Lyons, G. S. Engel, N. Balci, D. P. Schrag, B. Brunner. Kinetic oxygen isotope effects during dissimilatory sulfate reduction: a combined theoretical and experimental approach. *Geochim. Cosmochim. Acta.* **2010**, *74*, 2011.
[25] U. G. Wortmann, B. Chernyavsky, S. M. Bernasconi, B. Brunner, M. E. Böttcher, P. K. Swart. Oxygen isotope biogeochemistry of pore water sulfate in the deep biosphere: dominance of isotope exchange reactions with ambient water during microbial sulfate reduction (ODP Site 1130). *Geochim. Cosmochim. Acta.* **2007**, *71*, 4221.
[26] T. Boschetti, P. Iacumin. Continuous flow $\delta^{18}O$ measurements: new approach to standardization, high temperature thermodynamics and sulfate analysis. *Rapid Commun. Mass Spectrom.* **2005**, *19*, 3007.
[27] F. Fourel, F. Martineau, C. Lécuyer, H. J. Kupka, L. Lange, C. Ojeimi, M. Seed. $^{18}O/^{16}O$ ratio measurements of inorganic and organic materials by elemental analysis - pyrolysis - isotope ratio mass

spectrometry continuous - flow techniques. *Rapid Commun. Mass Spectrom.* **2011**, *25*, 2691.
[28] J. K. Böhlke, S. J. Mroczkowski, T. B. Coplen. Oxygen isotopes in nitrate: new reference materials for ^{18}O: ^{17}O: ^{16}O measurements and observations on nitrate - water equilibration. *Rapid Commun. Mass Spectrom.* **2003**, *17*, 1835.
[29] Z. D. Sharp, V. Atudorei, T. Durakiewicz. A rapid method for determination of hydrogen and oxygen isotope ratios from water and hydrous minerals. *Chem. Geol.* **2001**, *178*, 197.
[30] M. Gehre, G. Strauch. High - temperature elemental analysis and pyrolysis techniques for stable isotope analysis. *Rapid Commun. Mass Spectrom.* **2003**, *17*, 1497.
[31] S. F. Crowley, H. J. Spero, D. A. Winter, H. J. Sloane, I. W. Croudace. Oxygen isotope analysis of carbonates in the calcite - dolomite - magnesite solid - solution by high - temperature pyrolysis: initial results. *Rapid Commun. Mass Spectrom.* **2008**, *22*, 1703.
[32] H. P. Sieper, H. J. Kupka, L. Lange, A. Roβmann, N. Tanz, H. L. Schmidt. Essential methodological improvements in the oxygen isotope ratio analysis of N - containing organic compounds. *Rapid Commun. Mass Spectrom.* **2010**, *24*, 2849.
[33] A. Gygli. Microdetermination of oxygen in organic compounds using a glassy carbon pyrolysis tube and nondispersive infrared detection. *Microchim. Acta.* **1993**, *111*, 37.
[34] J. Unterzaucher. The direct micro-determination of oxygen in organic substances. *Analyst.* **1952**, *77*, 584.
[35] I. J. Oita, H. S. Conway. Direct determination of oxygen in organic substances modified Schütze method. *Anal. Chem.* **1954**, *26*, 600.
[36] R. N. Clayton, S. Epstein. The relationship between $^{18}O/^{16}O$ ratios in coexisting quartz, carbonate, and iron oxides from various geological deposits. *J. Geophys. Res.* **1958**, *66*, 352.
[37] E. Pella, B. Colombo. Improved instrumental determination of oxygen in organic compounds by pyrolysis - gas chromatography. *Anal. Chem.* **1972**, *44*, 1563.
[38] F. B. Wiedemann. Bidlack, A. S. Colman, M. L. Fogel. Phosphate oxygen isotope analysis on microsamples of bioapatite: removal of organic contamination and minimization of sample size. *Rapid Commun. Mass Spectrom.* **2008**, *22*, 1807.
[39] D. R. Lide. *CRC Handbook of Chemistry and Physics*, 87th ed, CRC press: Taylor and Francis, Boca Raton, FL, **2007**.

